



Improvement of a Flanged Diffuser Augmented Wind Turbine Performance by Modifying the Rotor Blade Aerodynamic Design

Open
Access

Balasem Abdulameer Jabbar Al-Quraishi^{1,2,*}, Sofian Mohd¹, Aghssan Mohammed Nwehil², Nor Zelawati Asmuin¹, Mohammed N. Nemah^{1,2}, Dhafer M. Hachim², Hyder H. Balla², Salih Meri¹, M. N. Hidayat¹

¹ Faculty of Mechanical and Manufacturing Engineering, University Tun Hussein Onn Malaysia (UTHM), Batu Pahat, Johor, Malaysia

² Engineering Technical College -Najaf, Al-Furat Al-Awsat Technical University, Najaf, Iraq

ARTICLE INFO

ABSTRACT

Article history:

Received 22 February 2020

Received in revised form 5 May 2020

Accepted 7 May 2020

Available online 8 June 2020

Shrouding of HAWT in a flanged diffuser is among techniques of wind power augmentation especially in urban areas. In this paper, a small scale of Flanged Diffuser Augmented Wind Turbine (FDAWT) was presented with flanges angle (Θ_f) of 0° . The rotor fit for FDAWT was designed based on a modified blade element momentum theory, which adopts on developing the preliminary rotor blade geometry in terms of pitch angle. The modification of the blade pitch angle was based on the maximum wind speeds in the empty flanged diffuser at rotor position along the blade sections. The models of rotor and diffuser were fabricated and experimented in the wind tunnel. The experimental tests were conducted to calculate the power at a different wind velocity ranged 5 - 9 m/s. The performance tests were in terms of power coefficient, C_p and torque coefficient, C_Q as a function of the tip speed ratio as well as maximum power as a function of the wind velocity. The results show the rate of increase in the maximum power producing for the FDAWT with the modified rotor up to 291% more than what it is for the preliminary bare HAWT, while this increase was only 257% for FDAWT with the preliminary rotor.

Keywords:

Wind Energy harvesting; HAWT; DAWT; FDAWT

Copyright © 2020 PENERBIT AKADEMIA BARU - All rights reserved

1. Introduction

Wind turbines represent the focus of researchers and scientists to produce power from wind for decades. Flowing of wind through the turbine rotor leads to the production of mechanical energy that can be used in many applications specially to produce electricity. However, power produced by wind turbine is dependent on the Betz limit; an ideal type can extract only 59.3% of incoming energy [1-2].

* Corresponding author.

E-mail address: balasemalquraishi@atu.edu.iq

<https://doi.org/10.37934/arfmts.72.1.124137>

Various types of wind turbine exist in different sizes, Horizontal axis wind turbine (HAWT) is one of these types. HAWT that have a rotor diameter of 1.25 m or less called a micro wind turbine. This type of turbine can be used to produce power in urban areas [3-4]. Several studies have been conducted to predict and develop the performance of HAWT. Some of these studies have been carried out either practical tests or simulation. Improving of HAWT performance can achieved by shrouded the turbine in a diffuser in this case it's called Diffuser Augmented Wind Turbine (DAWT) [5]. Many studies were conducted in this field, the augmentation of power factor was achieved of 2 to 5 [6]. The power coefficient and optimum tip speed ratio (λ) for DAWT much higher than bare turbine. The reason of tip speed ratio increases because increase of mass flow rate through rotor plane, where this increase produced from the pressure drop at diffuser outlet, so the rotor needs to rotating with a higher rpm [6]. Since DAWT performance enhancement depends on several factors including the diffuser shape and geometries, the diffuser parameters design are most important factors affected on the performance [7-8]. The diffuser with a flange at the exit at the proper height can increase wind velocity hence augmented the power of DAWT. So, the results of experimental and simulation study of small DAWT prove the power augmentation of DAWT-with flange reach to 1.58 higher than DAWT-without flange while it reached 2.8 over bare HAWT for the same rotor [9]. The DAWT studies have not only developed the distributor's parameters but have also gone beyond that. Some studies have focused on re-designing rotor blade suitable for the DAWT design which is a bit like the behavior of conventional studies to develop bare HAWT as in Jabbar and Sanke [10] and El khchine and Sriti [11] that adopted the blade element momentum (BEM) theory. Improving rotor blade geometry is one of the factors that controlled the DAWT performance so, in a study to optimize the rotor design by Van Dorst [12] through present a two developed design of blade (optimal and linearized), the power measurements showed that the power coefficient of the DAWT with the developed blade is increased with 15% over the DAWT with old blade. Fletcher [13] developed BEM computational analysis including wake rotation and blade Reynolds number effects, and introduces two empirical parameters: the exit pressure coefficient and the diffuser efficiency, to incorporate the influence of the diffuser into the analysis. With that approach, he obtained good agreement for power coefficient and turbine axial velocity with experimental results. The 1D mathematical model presented by do Rio *et al.*, [14] which adopt an extended in BEM theory for blade design suitable for DAWT, where it is possible to evaluate the performance of the wind turbine under the effect of the diffuser, considering the geometry of the wind blade. The model had low computational cost due to the fact of being based on the BEM model and presents good agreement with experimental data. In the own previous study [9], the model of flanged diffuser augmented wind turbine (FDAWT), which was flanged diffuser that encloses the bare HAWT rotor (preliminary rotor), which was designed adopted the conventional BEM theory.

In the present paper, theoretical design and the experimental test was carried out to study the performance of a small scale DAWT with the best configuration for the flanged diffuser and according to the modified BEM theory for rotor design (modified rotor). The experiments performance was in terms of power, power coefficient, and torque coefficient. The study also included a comparison for the performance of flanged diffuser augmented wind turbine with modified rotor (DAWT-MR) to the previous models of a flanged diffuser augmented wind turbine with preliminary rotor (DAWT-PR) and Bare HAWT (BHAWT) presented in the previous study.

2. Methodology

2.1 Mathematical Model

Several studies have focused on the development of wind turbine performance through development of BEM theory and have undergone some modifications to improve power [15]. But in case of enclosing wind turbine in a duct, which is called diffuser augmented wind turbine (DAWT), some researchers used the conventional BEM theory, while others took into account the effect of thrust (due to in the presence of the duct) on the BEM theory.

2.1.1 Adoption of conventional BEM theory

In the previous study [9], the HAWT was enclosed by a flanged diffuser, where the rotor blade was designed based on the conventional BEM theory (for the bare turbine) which is combined of classic momentum and blade element theory. The classical momentum theory was represented the wind turbine as actuator disk based on assumptions as: incompressible, steady flow, no friction, infinite of blades, uniform thrust over the disk, non- rotating wake, and undisturbed ambient static pressure for far-field flow [16]. The classical momentum control volume of bare HAWT are shown in Figure 1. The velocities V_1 and V_d at the disc and in the wake, respectively are written respect to upstream wind velocity, V_∞ (m/s) as follow:

$$V_1 = V_2 = V_\infty(1 - a) \quad (1)$$

$$V_d = V_\infty(1 - 2a) \quad (2)$$

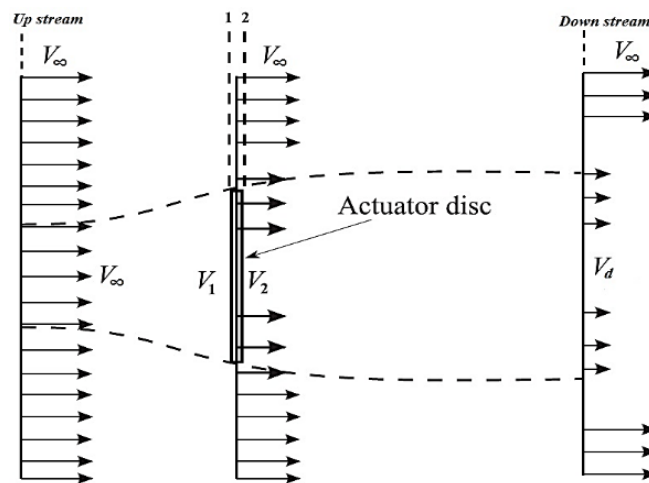


Fig. 1. Classical momentum control volume [16]

The angle of relative wind (φ) based on conventional BEM theory can be calculated from Figure 2 as follow in Eq. (3), where a and a_t Axial and tangential induction factor for bare turbine, Ω is Angular velocity of the rotor (rad / s) and r is Radial position (m).

$$\tan(\varphi) = \frac{V_\infty(1-a)}{\Omega r(1+a_t)} \quad (3)$$

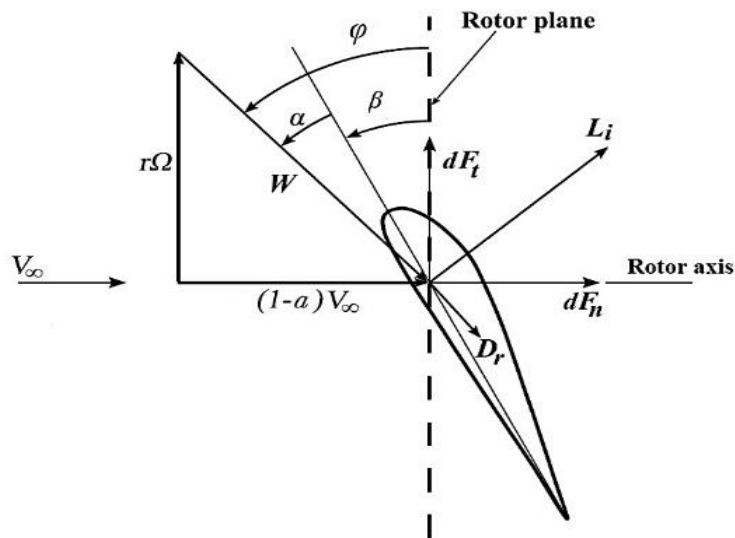


Fig. 2. Blade section geometry definition based on conventional BEM theory [16]

2.1.2 Adoption of modified BEM theory

In this study the design of HAWT suitable for DAWT done depends on extension BEM theory presented by do Rio *et al.*, [14] which considered effect of diffuser on performance of wind turbine, which is required a develop in blade profile to be suitable for DAWT, so this theory adopted a modifying the blade in terms of pitch angle with maintaining the other parameters. The classical theory with diffuser a similar formulation is used with considering losses through the diffuser. Figure 3 shows the control volume for the actuator disc with diffuser.

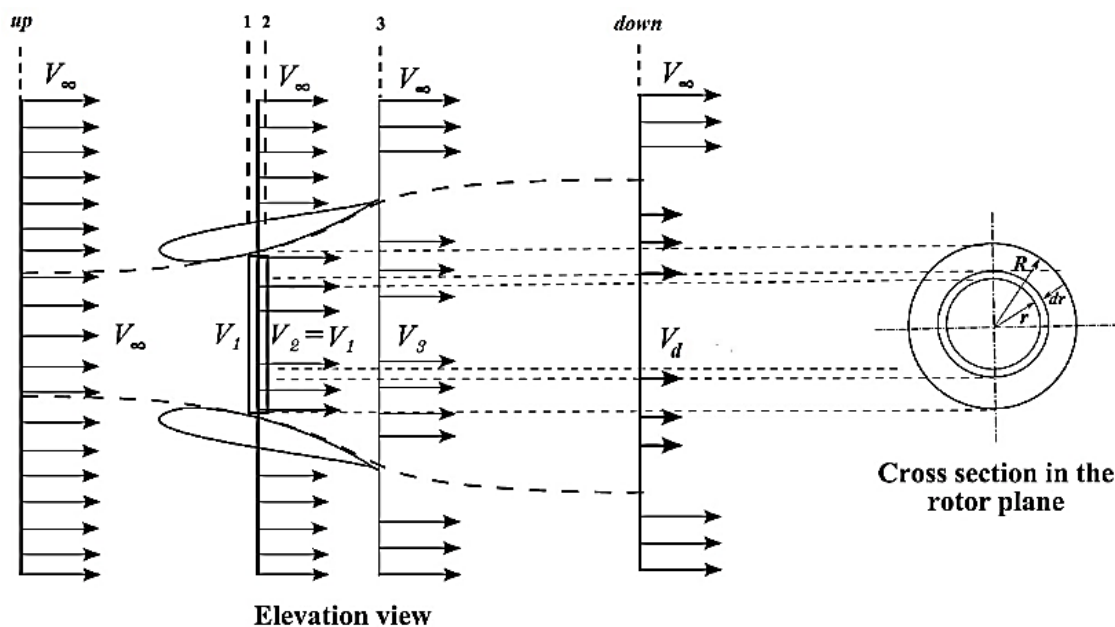


Fig. 3. The disc actuator control volume enclosing by diffuser [14]

Shrouding the turbine rotor by a diffuser causing an increase in mass flow through the rotor due to pressure drop downstream, therefore resulting in an increase in velocity arriving at the rotor.

Figure 4 illustrates a typical velocity profile on the symmetry axis of a diffuser without the turbine, ϵ , is ratio of maximum axial velocity at empty diffuser (V_1^*) to upstream velocity (V_∞).

$$\epsilon = \frac{V_1^*}{V_\infty} \quad (4)$$

From Figure 3, the velocities V_1 and V_d at the disc and in the wake, respectively, are written as

$$V_1 = V_2 = V_\infty(1 - a^*)\epsilon \quad (5)$$

In case no losses in diffuser, V_d calculate as

$$V_d = V_\infty(1 - 2a^*) \quad (6)$$

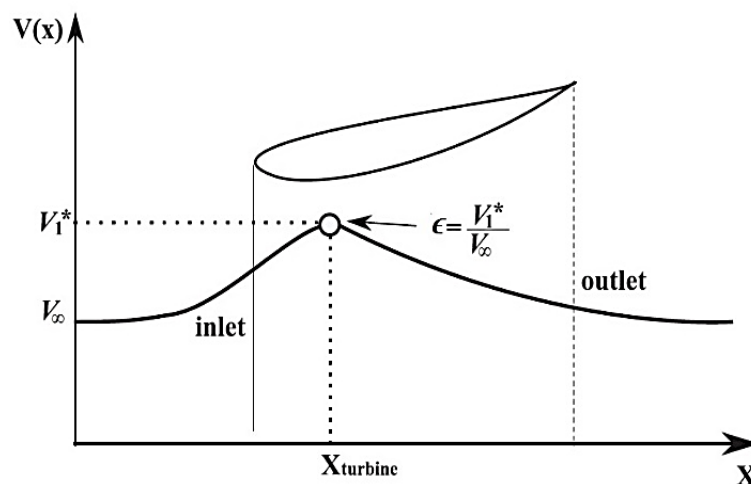


Fig. 4. Axial velocity profile of a diffuser without turbine [14]

Based on Figure 5, φ based on modified BEM theory are

$$\tan(\varphi) = \left[\epsilon \frac{V_\infty(1-a^*)}{\Omega r(1+a_t^*)} \right] \quad (7)$$

where: a^* and a_t^* are Axial and tangential induction factor for wind turbine with diffuser (DAWT)

From Figure 2 and Figure 5, the pitch angle (β) of the blade is defined in Eq. (8), where α is Angle of attack (deg).

$$\beta = \varphi - \alpha \quad (8)$$

The coefficients of normal (C_n) and tangential forces (C_t) are defined by Eq. (9) and Eq. (10), where C_L and C_D are lift and drag coefficient

$$C_n = C_L \cos(\varphi) + C_D \sin(\varphi) \quad (9)$$

$$C_t = C_L \sin(\varphi) - C_D \cos(\varphi) \quad (10)$$

The axial and tangential induction factors for DAWT determined by

$$a^* = \frac{\epsilon^2 \sigma C_n}{4 \sin^2(\varphi) + \epsilon^2 \sigma C_n} \quad (11)$$

$$a_t^* = \frac{\sigma C_t}{4 \sin(\varphi) \cos(\varphi) - \sigma C_t} \quad (12)$$

where σ is blade solidity defined in Eq. (13) as function of number of blade (B) and chord length(c).

$$\sigma = \frac{Bc}{2\pi r} \quad (13)$$

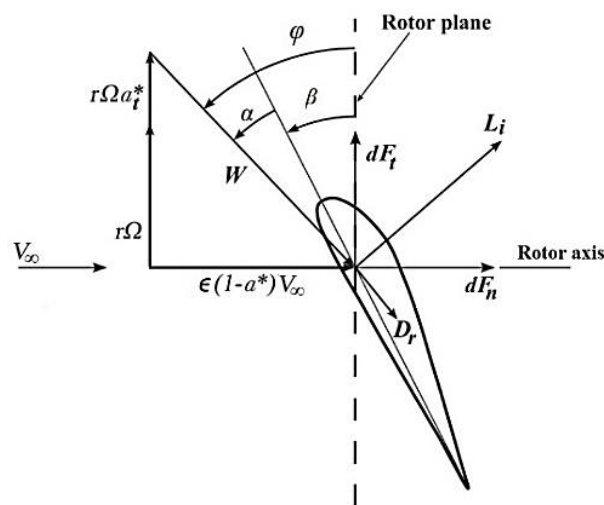


Fig. 5. Blade section geometry definition based on modified BEM theory [14]

2.2 Description of DAWT Model

The model of DAWT in this study is consist of HAWT shrouded by flanged diffuser, which it is called flanged diffuser augmented wind turbine [9]. The turbine rotor is a small-scale of 1:6.5 with three blades of NACA SD8000 [17]. Thus, the parameters design of turbine model is shown in Table 1.

Table 1

The main parameters of rotor design

Rotor diameter (D_r)	15.4 cm
Hub diameter (D_h)	2.61 cm
Blade span length (l)	6.39 cm
Blade root length (l_r)	0.92 cm
Number of blades (B)	3
Number of elements per blade	10
element radial distance (d_r)	0.77 cm
Airfoil type	NACA SD8000
Angle of attack (α)	5°
Design tip speed ratio (λ_d)	5
Design wind velocity (V_∞) _d	10 m/sec

The diameter and length of diffuser that used to shroud the turbine are 16 cm and 8 cm respectively with expansion angle of 12° , 3mm wall thickness and flange height of 3.2 cm at two configurations of flange angle 0° and 5° as presented in a previous study [8]. The best performance for the diffuser was found out with flange angle of 0° , so this design was adopted to calculate the ϵ value at ten sections along of blade at the position of turbine rotor based on the 2- D CFX, which was adopted in own previous study [8] as shown in Figure 6. The diffuser was placed at 60 cm from inlet test domain. No slip wall, for a diffuser and bottom domain were considered, as well as the model is symmetric about the axis.

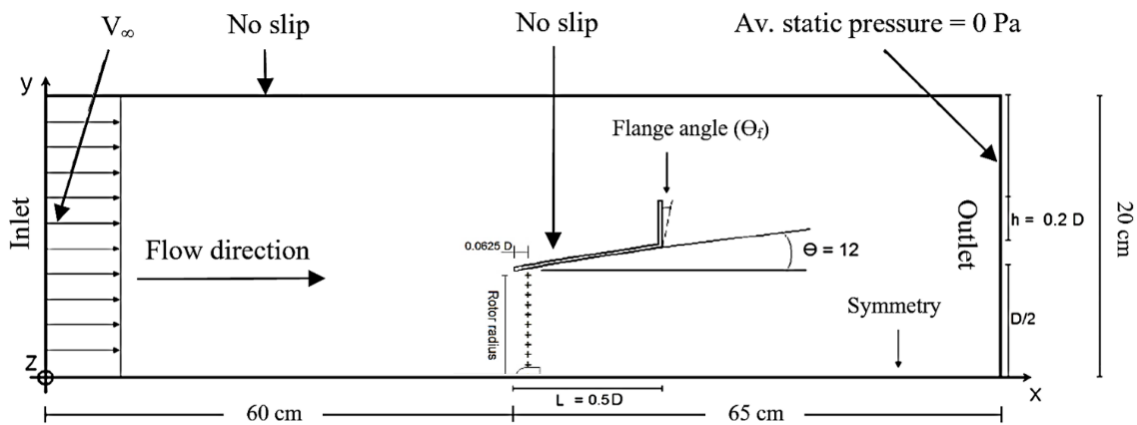


Fig. 6. The 2-D axisymmetric simulation domain for the flanged diffuser

The procedure for design calculation of modified rotor blade for each radial section along the blade are based on the equations that mention above using Mat lab program and define the parameters of (V_∞ , r , $c(r)$, $\epsilon(r)$, α , C_L and C_D) which considered same whose in preliminary rotor blade. The programming steps of calculation the pitch angle of modified blade was be as following.

- i. Define the initial values of $a^* = 1/3$ and $a_t^* = 0$.
- ii. Calculate φ by using Eq. (7)
- iii. Calculate C_n and C_t using Eq. (9) and Eq. (10)
- iv. Calculate new values of a^* and a_t^* using Eq. (11) and Eq. (12)
- v. Calculate error $|\varphi_{iter+1} - \varphi_{iter}|$
- vi. Calculate β using Eq. (8)
- vii. Table 2 illustrate the design parameters of the blade for the preliminary rotor (PR) and modified (MR) rotor blade included the values of the ratio of maximum axial to upstream wind velocity (ϵ) in the diffuser for each element.

Table 2

The geometry design parameters of preliminary rotor (PR) and modified rotor (MR) blade

section	r/R	Chord length (c) (cm)	Pitch angle (β)-PR (deg)	ϵ	Pitch angle (β)-MR (deg)
1	0.2	2.36	25	1.45875	31.3
2	0.29	2.05	18.1	1.46304	23.8
3	0.38	1.74	13.6	1.47079	19.6
4	0.47	1.48	10.5	1.48291	16.2
5	0.56	1.29	8.2	1.50222	13.6
6	0.64	1.14	6.5	1.53136	12
7	0.73	1.02	5.2	1.57422	10.5
8	0.82	0.91	4.1	1.68492	9.9
9	0.91	0.83	3.3	1.73168	8.8
10	1	0.77	2.5	1	2.5

These data were used to redesign of rotor blade suitable to DAWT. The difference between modified and preliminary rotor blade was in the geometry design in term of pitch angle (β) so, Figure 7 shows the comparison for the pitch angle between the two rotor blades from root to tip, in same manner of Marco Torresi [18]. It can be observed an increase in β for the modified blade compare to preliminary one. The increase was along of the element section except the last section at the tip, it remains at same as preliminary design due to ϵ value at this section is equals 1. Since the increase of wind velocity at the rotor plane causes an increase in the angle of relative wind (φ), hence the pitch angle must be increased, with a constant angle of attack (α) was considered. Moreover, the increase of blade twisting help to rotating the rotor faster as possible.

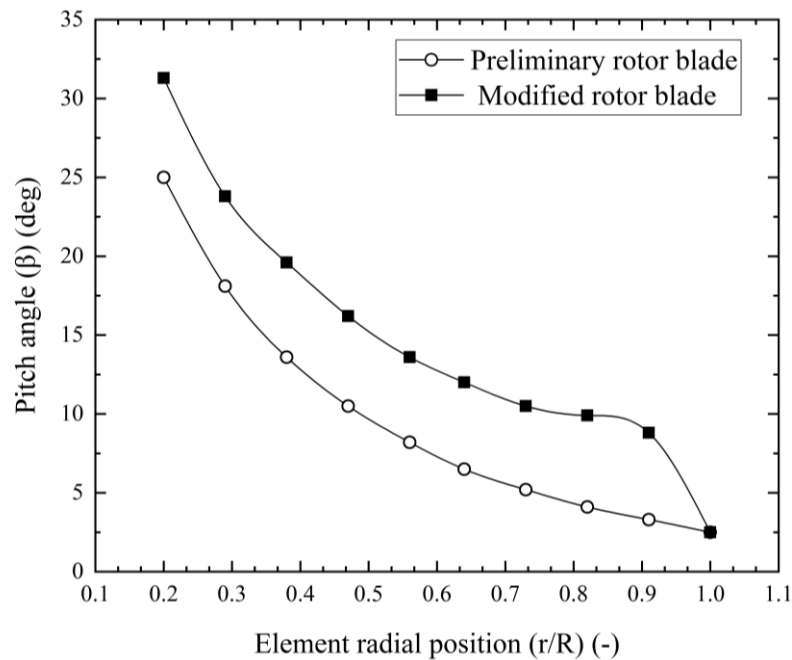


Fig. 7. Comparison of pitch angle for the modified and preliminary rotor blade

2.3 Experimental Set Up

The prototypes of rotor (containing three blades and hub) and flanged diffuser were modelled using Solid Work 2017, then they manufactured from RGD450 material using polyjet 3D printing technology as describe in Figure 8. The wind tunnel of Aerodynamic Lab, Faculty of Mechanical Engineering and Manufacturing (FKMP), UTHM with test section of 125 cm \times 40 cm \times 40 cm is used which can produced a maximum wind velocity of 40 m/s. The FDAWT is placed at a distance of 60 cm from test section inlet [17]. The turbine is attached to a 3-phase AC 12-Watt alternator generator which connected to a 6- diode full wave rectifier to convert the suppling power to a 1-phase DC [17], [15], and [9]. The FLUKE 922 digital Airflow Meter with Pitot tube used to measure the velocity and pressure of inlet air [19]. The angular velocity of the wind turbine was measured using non-contact type, digital Tachometer 'DT-2234B' (RS 445-9557) [20]. The power calculations of FDAWT were performed using A load control board that has been used in own previous study [17]. In this board, 16 of 12V, 1-Watt LEDs load were utilized and connected as a series electrical circuit. Since the power generated is equal to multiplier voltage into the current, tow of ANEGN AN8002 AC/DC Digital Multi-meters connected directly across the output power of the generator to record the voltage and the current for each loading case [21]. The experimental setup is shown in Figure 9. The generator of the

turbine is connected to load; the voltmeters were used to measure the voltage and current across the load. By maintaining air velocity is constant, the load can be varied by operating more load (LEDs), the voltage and current were recorded at each load. At the same time, the angular velocity is recorded at each load. The experiment was repeated several times based on cases of the models. The experiments for the model of FDAWT with MR was conducted and compared to the model of FDAWT with PR at wind speed in the range from 5 to 9 m/s.

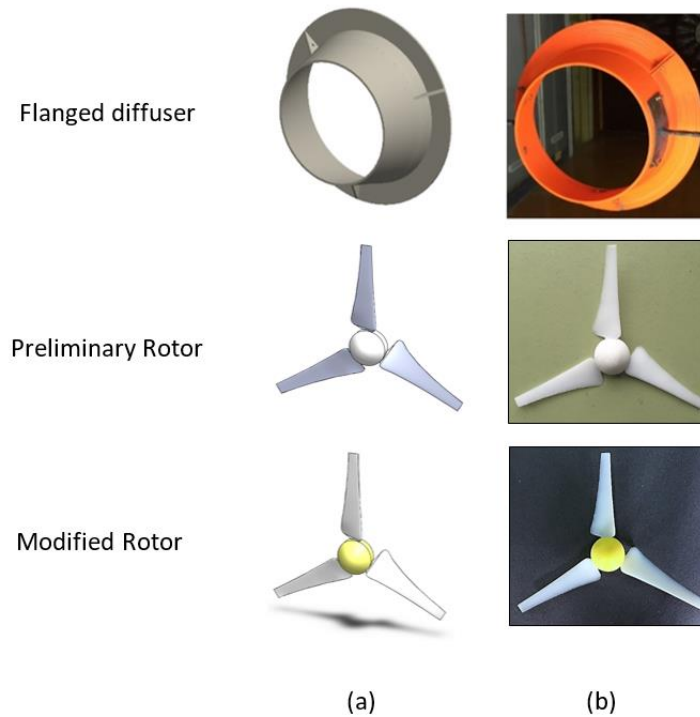


Fig. 8. FDAWT (Rotor and flanged diffusers models) (a) modelling models, (b) prototype models

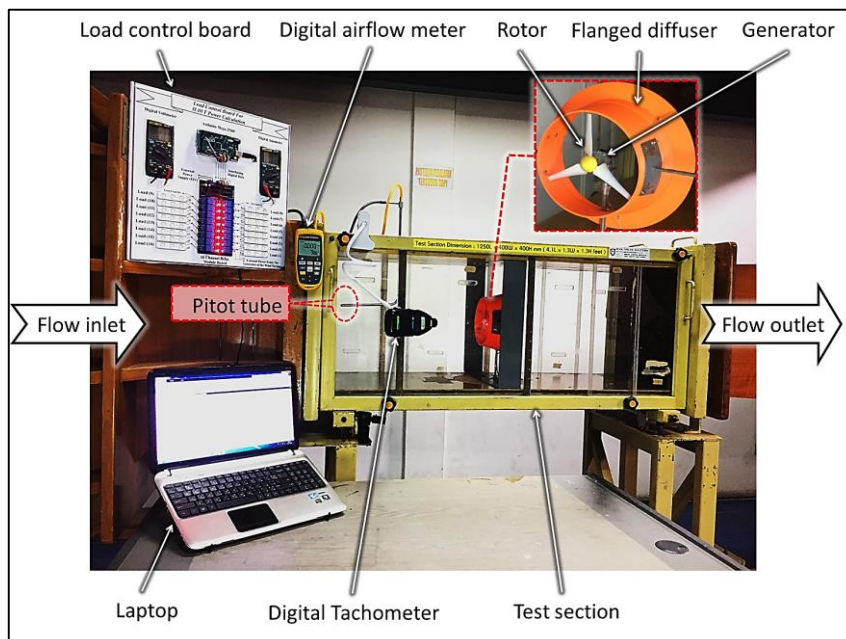


Fig. 9. The experimental set up testing of FDAWT

Since wind power is source the mechanical power of wind turbine, which is the product of rotor torque and angular velocity of rotor. So, the wind turbine performance is represented by the power coefficient (C_p) which is defined as

$$C_p = \frac{P_{out}}{P_{wind}} = \frac{Q\Omega}{0.5 \rho A V_{\infty}^3} \quad (14)$$

The most common method used to preview the power coefficient by graphing its values as function with tip speed ratio (λ) which is defined as

$$\lambda = \frac{\Omega R}{V_{\infty}} \quad (15)$$

Moreover, torque coefficient (C_Q) can be considered as parameters for study turbine performance, especially for DAWT [22-23]. Thus, C_Q as a function of C_p defined as

$$C_Q = \frac{\text{Actual torque}}{\text{Theoretical torque}} = \frac{Q}{0.5 \rho A R V_{\infty}^2} = \frac{C_p}{\lambda} \quad (16)$$

where Q is actual rotor torque (N.m), Ω is angular velocity (rad/s), ρ air density (kg/m^3), A is rotor swept area, V_{∞} is upstream wind velocity, and R is rotor radius.

3. Results and Discussion

The practical tests were performed to calculate the aerodynamic performance characteristics of the turbine. Thus, the experimental tests have been performed to calculate the aerodynamic performance characteristics of the turbine, of which most importantly, the power and turbine coefficients. Although the turbine models designed in this study works within a different range of upstream wind velocities including low speeds but the models were tested with a specific range of speeds from 5 to 9 m/s. This range of speeds was considered for reasons, they are, the generator used in the experiment difficult to start a rotation with low velocity less than 5, on the other hand, high speed over 9 m/s may cause a break in rotor blades.

The mechanical power (P_{out}) of FDAWT was calculated experimentally from the voltage and current recorded at each load with considering values for the mechanical and conversion efficiencies for the generator. The angular velocity can be measured experimentally using tachometer in rpm, so the actual torque can be calculated.

The coefficient of the turbine is usually expressed as a function of tip speed ratio, λ which is varying with rpm of a rotor. As such, the current study expressed of the performance in terms of power coefficient, C_p and torque coefficient C_Q . Two velocities 7 and 8 m/s were chosen for determining these two coefficients (C_p and C_Q) as a function of tip speed ratio for the configuration of FDAWT-MR ($\Theta_f = 0^\circ$) compare to FDAWT-PR ($\Theta_f = 0^\circ$). Figure 10 and Figure 11 show the power coefficient as function of λ at upstream wind velocity of 7 m/s and 8 m/s respectively. As can be seen from plots, the power coefficient is increased as tip speed ratio increase until reach to a maximum value, then trend to a little decrease because the rotor when rotate fast appear like air disk, so the air is passed through it with less effect. The analysis of power coefficient can be used to observe for torque coefficient analysis as in Figure 12 and Figure 13 at wind velocity of 7 m/s and 8 m/s respectively. This is due to the torque coefficient is a function of power coefficient for the same tip speed ratio. It has been observed from these figures that there is a marked increase in the amount

of C_p and C_Q in the DAWT- MR model as compare to their counterparts in DAWT-PR and It is also more stable especially for C_Q values.

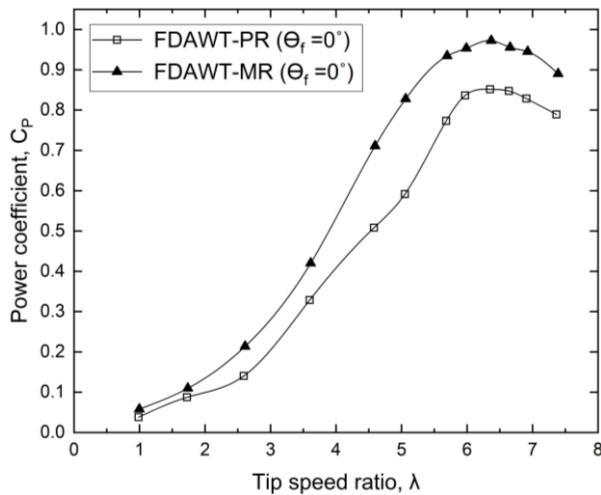


Fig. 10. Power coefficient as a function of tip speed ratio at a wind speed of 7 m/s for FDAWT - MR compare to FDAWT-PR

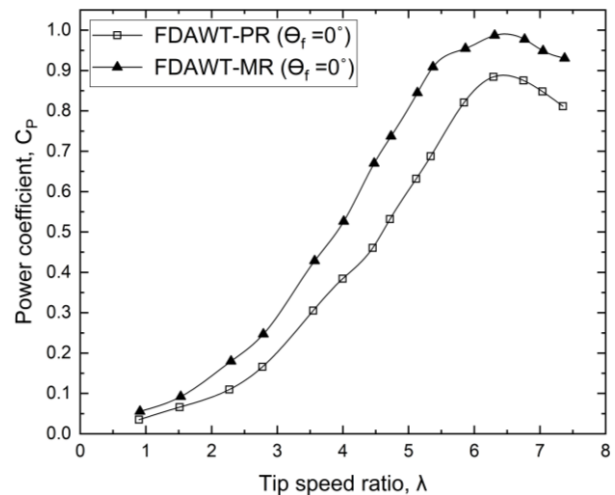


Fig. 11. Power coefficient as a function of tip speed ratio at a wind speed of 8 m/s for FDAWT - MR compare to FDAWT-PR

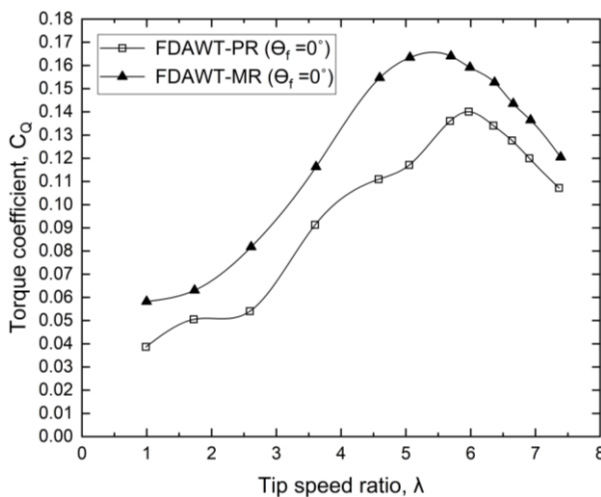


Fig. 12. Torque coefficient as a function of tip speed ratio at a wind speed of 7 m/s for DAWT - MR compare to FDAWT-PR

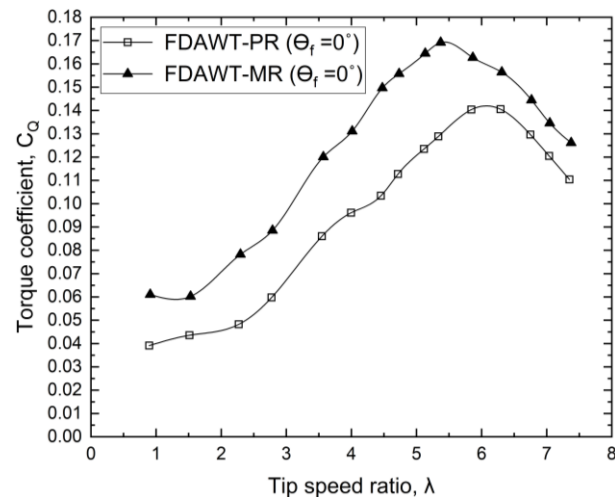


Fig. 13. Torque coefficient as a function of tip speed ratio at a wind speed of 8 m/s for DAWT - MR compare to FDAWT-PR

The second criteria to represent of power coefficient and torque coefficient as mention above is by adopted the maximum values of C_p and C_Q respect to wind velocity in the range of 5 to 9 m/s, as shown in Figures 14 and 15. By analyzing the figures one after the other, in Figure 14 it can observe that the value of the C_p for FDAWT-MR ($\Theta_f = 0^\circ$) are increase by increasing the velocity of the wind from the range of 5 to 7, then it was inclined to stability unlike FDAWT-PR ($\Theta_f = 0^\circ$) that is wobbly. The model of FDAWT-MR ($\Theta_f = 0^\circ$) continues to maintain the highest of average C_p at 0.952 compare to that calculated for FDAWT-PR ($\Theta_f = 0^\circ$) which was only 0.869. Figure 15 shows the torque coefficient, C_Q as a function to tip speed ratio. The graph exhibits the same behavior of C_p because the torque coefficient is related to power coefficient. Generally, it turns out that the DAWT-MR has been achieving a significant increase in C_p and C_Q compare to DAWT-PR.

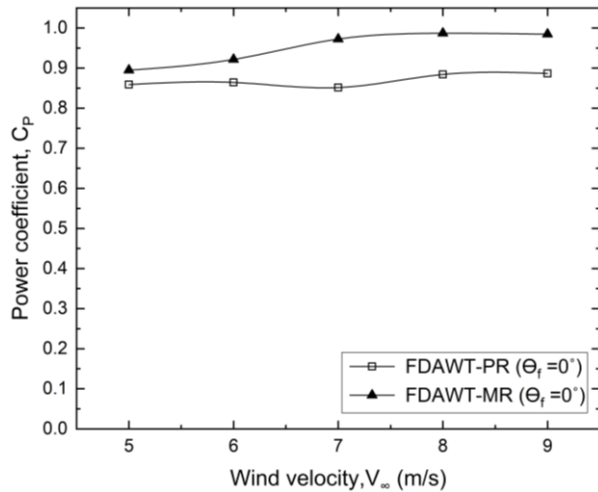


Fig. 14. Maximum power coefficient as a function of wind velocity for DAWT - MR compare to FDAWT-PR

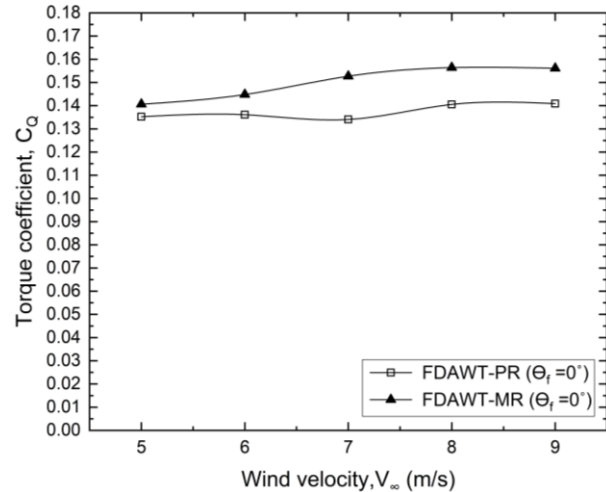


Fig. 15. Maximum torque coefficient as a function of wind velocity for DAWT - MR compare to FDAWT-PR

Furthermore, it must be mentioned the performance of model design of FDAWT-MR ($\Theta_f = 0^\circ$) compare to FDAWT-PR ($\Theta_f = 0^\circ$) and bare horizontal axis wind turbine (BHAWT) in terms of power producing. The maximum power output as a function to wind velocity in the range of 5 to 9 m/s is illustrated in Figure 16 of the two models compare to the preliminary bare turbine model. It is evident that the models of FDAWT at ($\Theta_f = 0^\circ$) with preliminary and modified rotor showed a significant increase in power output compare to BHAWT. As wind velocity increases, the power output increase of all models, but it is noticed that there is a boost in this increasing for the FDAWT-MR compared to the others. The increase in the power output ratio of FDAWT-PR model at the wind velocity of 5 m/s up to about 283.3% while it is reaching 299.4% for FDAWT-MR model at the same velocity condition. At the wind velocity of 9 m/s, the maximum increase in power is about 262.3% in FDAWT-PR model compared to BHAWT, while this increase up to 286.2% at FDAWT-MR model. In general, the rate of increase in the maximum power producing of the FDAWT-PR model is 257%, while it is 291% for FDAWT-MR model. Moreover, Figure 16 illustrated the maximum augmentation ratio of power ($P_{\text{FDAWT}(\Theta_f=0^\circ)\text{-MR}} / P_{\text{BHAWT-PR}}$) in an average of 3.91.

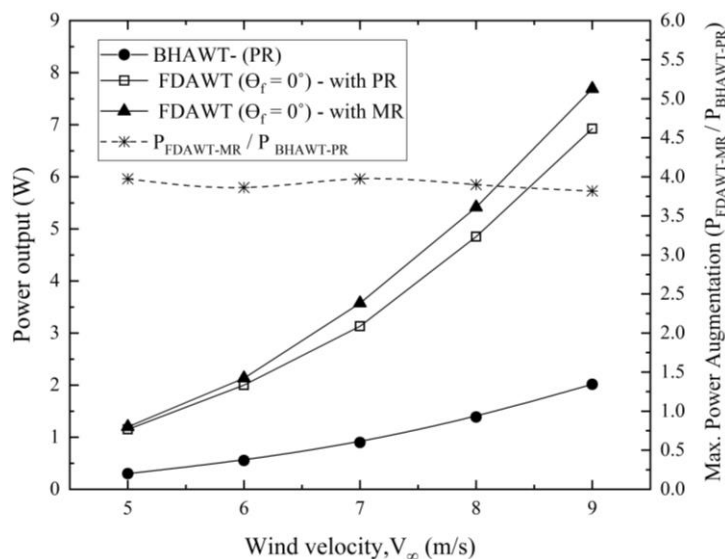


Fig. 16. Comparison between FDAWT-MR and FDAWT-PR relative to BHAWT

4. Conclusion

In this paper, a small scale of FDAWT was presented with flanges angle (θ_f) of 0° . Due to the increments of wind velocity in the diffuser (at rotor position) was not considered at the preliminary rotor blade design, the blade geometry was developed to be more convenient for FDAWT. The rotor blade design was adopted a modified blade element momentum theory based on developing the blade geometry in terms of pitch angle. The theoretical result of the redeveloped rotor blade shows that the modified blade has pitch angles along the blade greater than the preliminary blade. The experimental tests were conducted at wind tunnel to calculate the power at a different wind velocity ranged 5 - 9 m/s. the results show the rate of increase in the maximum power producing for the FDAWT-MR up to 291% more than what it is for the preliminary bare HAWT, where this ratio increase is much more what is in the model of FDAWT-PR. these increase due to wind velocity increase at the rotor plane, Moreover, the increase of blade twisting (pitch angle) help to rotating the rotor faster as possible and increase the torque, hence more power produced.

Acknowledgement

The authors are thankful to the staff of Aerodynamic Lab, Faculty of Mechanical and Manufacturing Engineering, UTHM, Malaysia. They are also grateful to Mr. Encik Ghazali Bin Kadis, mechanical engineer in UTHM who provided the expertise that greatly assisted the research.

References

- [1] Libii, Josué Njock, and David M. Drahozal. "The influence of the lengths of turbine blades on the power produced by miniature wind turbines that operate in non-uniform flow fields." *World Trans. Eng. Technol. Educ* 10, no. 2 (2012): 128-133.
- [2] Igra, Ozer. "Research and development for shrouded wind turbines." *Energy Conversion and Management* 21, no. 1 (1981): 13-48.
[https://doi.org/10.1016/0196-8904\(81\)90005-4](https://doi.org/10.1016/0196-8904(81)90005-4)
- [3] Peacock, A. D., D. Jenkins, M. Ahadzi, A. Berry, and S. Turan. "Micro wind turbines in the UK domestic sector." *Energy and Buildings* 40, no. 7 (2008): 1324-1333.
<https://doi.org/10.1016/j.enbuild.2007.12.004>
- [4] Gipe, Paul. *Wind energy basics*. Chelsea Green Pub. Co., 1999.
- [5] Alquraishi, Balasem Abdulameer, Nor Zelawati Asmuin, Sofian Mohd, Wisam A. Abd Al-Wahid, and Akmal Nizam Mohammed. "Review on Diffuser Augmented Wind Turbine (DAWT)." *International Journal of Integrated Engineering* 11, no. 1 (2019).
- [6] Ohya, Yuji, Takashi Karasudani, Tomoyuki Nagai, and Koichi Watanabe. "Wind lens technology and its application to wind and water turbine and beyond." *Renewable Energy and Environmental Sustainability* 2 (2017): 2.
<https://doi.org/10.1051/rees/2016022>
- [7] Jafari, Seyed AH, and Buyung Kosasih. "Flow analysis of shrouded small wind turbine with a simple frustum diffuser with computational fluid dynamics simulations." *Journal of Wind Engineering and Industrial Aerodynamics* 125 (2014): 102-110.
<https://doi.org/10.1016/j.jweia.2013.12.001>
- [8] Al-Quraishi, Balasem Abdulameer Jabbar, Nor Zelawati Asmuin, Nurul Fitriah Nasir, Noradila Abdul Latif, Juntakan Taweekun, Sofian Mohd, Akmal Nizam Mohammed, and Wisam Abd al-wahid. "CFD Investigation of Empty Flanged Diffuser Augmented Wind Turbine." *International Journal of Integrated Engineering* 12, no. 3 (2020): 22-32.
<https://doi.org/10.36478/jeasci.2019.9162.9170>
- [9] Balasem Abdulameer Jabbar, Nor Zelawati Binti Asmuin, Sofian Bin Mohd, Mohammed Najeh Nemah, Salih Meri, and Mohamad Nur Hidayat Mat. "Influence of Flanged Diffuser on Diffuser Augmented Wind Turbine Performanc." *Journal of Engineering and Applied Sciences* 14, no. 24 (2019).
- [10] B. A. Jabbar, and N. Sanke. "Design and Modeling of Horizontal Axis Wind Turbine Blade." In *National Conference on Recent Advances in Mechanical Engineering*, UCE, OU, Hyderabad, no. March. 2012.
- [11] Sriti, Mohammed. "Performance prediction of a horizontal axis wind turbine using BEM and CFD methods." In *MATEC Web of Conferences*, vol. 45, p. 05005. EDP Sciences, 2016.

- <https://doi.org/10.1051/mateconf/20164505005>
- [12] van Dorst, F. A. "An Improved Rotor Design for a Diffuser Augmented Wind Turbine: Improvement of the DONQI URBAN WINDMILL." (2011).
- [13] Fletcher, Clive AJ. "Computational analysis of diffuser-augmented wind turbines." *Energy Conversion and Management* 21, no. 3 (1981): 175-183.
[https://doi.org/10.1016/0196-8904\(81\)90012-1](https://doi.org/10.1016/0196-8904(81)90012-1)
- [14] do Rio, Déborah Aline Tavares Dias, André Luiz Amarante Mesquita, Jerson Rogério Pinheiro Vaz, Claudio José Cavalcante Blanco, and João Tavares Pinho. "An extension of the blade element momentum method applied to diffuser augmented wind turbines." *Energy Conversion and Management* 87 (2014): 1116-1123.
<https://doi.org/10.1016/j.enconman.2014.03.064>
- [15] Lee, Meng-Hsien, Yui-Chuin Shiah, and Chi-Jeng Bai. "Experiments and numerical simulations of the rotor-blade performance for a small-scale horizontal axis wind turbine." *Journal of Wind Engineering and Industrial Aerodynamics* 149 (2016): 17-29.
<https://doi.org/10.1016/j.jweia.2015.12.002>
- [16] Manwell, James F., Jon G. McGowan, and Anthony L. Rogers. *Wind energy explained: theory, design and application*. John Wiley & Sons, 2010.
<https://doi.org/10.1002/9781119994367>
- [17] Balasem, A. Al-quraishi, Nor Zelawati Asmuin, M. N. Nemah, and Salih Meri AR. "Experimental and simulation investigation for performance of a small-scale model of bare and shrouded HAWT." *Int. J. Mech. Eng. Technol* 10, no. 1 (2019): 434-449.
- [18] Torresi, Marco, Nicolangelo Postiglione, Pasquale F. Filianoti, Bernardo Fortunato, and Sergio M. Camporeale. "Design of a ducted wind turbine for offshore floating platforms." *Wind Engineering* 40, no. 5 (2016): 468-474.
<https://doi.org/10.1177/0309524X16660226>
- [19] Fluke Corporation. *Fluke 922 Airflow Meter*. PN 2683880, User Manual, November 2006.
- [20] RS PRO. "Laser, Photo Tachometer." RS 445-9557, datasheet
- [21] ANEGN. "AN8002 AC/DC Digital Multi-meters." datasheet.
- [22] AR, Salih Meri, Mohammed Najeh Nemah, Balasem A. Al-Quraishi, and Nor Zelawati Binti Asmuin. "PERFORMANCE EVALUATION OF SAVONIUS WIND TURBINE BASED ON A NEW DESIGN OF BLADE SHAPE." *International Journal of Mechanical Engineering and Technology* 10, no. 1 (2019): 837-846.
- [23] Kosasih, Buyung, and H. Saleh Hudin. "Influence of inflow turbulence intensity on the performance of bare and diffuser-augmented micro wind turbine model." *Renewable Energy* 87 (2016): 154-167.
<https://doi.org/10.1016/j.renene.2015.10.013>